Journal of Paleontology, 90(1), 2016, p. 170–181

0022-3360/16/0088-0906
doi: 10.1017/jpa.2016.13

Journal of PALEONTOLOGY
A JOURNAL OF THE PALEONTOLOGICAL SOCIETY

A new anthracothere (Artiodactyla) from the early Oligocene, Fayum, Egypt, and the mystery of African '*Rhagatherium*' solved

Afifi H. Sileem,[1] Hesham M. Sallam,[2] Abdel Galil A. Hewaidy,[3] Ellen R. Miller,[4] and Gregg F. Gunnell[5]

[1]Vertebrate Paleontology Section, Cairo Geological Museum, Cairo, Egypt ⟨afifi.sileem@yahoo.com⟩
[2]Mansoura University Vertebrate Paleontology Center, Department of Geology, Mansoura University, Mansoura, 35516, Egypt ⟨sallam@mans.edu.eg⟩
[3]Department of Geology, Faculty of Science, Al-Azhar University, Egypt ⟨ahewaidy50@yahoo.com⟩
[4]Department of Anthropology, Wake Forest University, Winston-Salem, North Carolina 27106, USA ⟨millerer@wfu.edu⟩
[5]Division of Fossil Primates, Duke Lemur Center, Durham, North Carolina 27705, USA ⟨gregg.gunnell@duke.edu⟩

Abstract.—Recent work on new anthracothere (Mammalia, Artiodactyla) specimens from the Jebel Qatrani Formation, early Oligocene, Fayum, Egypt, has revealed the presence of a new genus. *Nabotherium* new genus is described on the basis of a partial skull, several mandibular and maxillary specimens, and isolated teeth. The new genus exhibits a distinctive combination of features not seen in other Paleogene anthracotheres. The most noticeable characteristics of the new genus include the presence of large and well-developed upper and lower canines, caniniform third incisors, the presence of only a short diastema between the canine and first premolar, and broad, bunodont cheek teeth. This is in contrast to other contemporary anthracotheres, including other forms from the Fayum, which show a spatulate third incisor, a reduced canine, a much longer canine-premolar diastema, and more narrow, bunoselenodont cheek teeth. The presence of a relatively short rostrum with closely packed incisors, low-crowned and simple premolars, and low-crowned, bunodont molars indicates that members of the new genus would have been more efficient at crushing foods than slicing vegetation, and suggests a more varied herbivorous and frugivorous diet than was favored by other, more bunoselenodont Fayum anthracotheres.

Introduction

Fossiliferous sedimentary deposits in the Fayum Depression, Western Desert, Egypt (Fig. 1) have produced a remarkable assemblage of late Eocene and early Oligocene animals, representing a wide variety of fish, amphibians, reptiles, birds, and mammals (e.g., Andrews, 1906; Rasmussen and Simons, 1988; Gingerich et al., 1990; Simons and Rasmussen, 1990; Domning and Gingerich, 1994; Domning et al., 1994; Seiffert et al., 2003, 2009; Seiffert, 2006, 2007, 2010, 2012; Simons et al., 2007; Sallam et al., 2009, 2011; Murray et al., 2010). Despite the fact that anthracotheres (Mammalia, Artiodactyla) are represented throughout most of the sequence (Fig. 2) and are among the most common faunal elements preserved in Fayum localities, very little has been published about the group since the early part of the twentieth century (Andrews, 1906; Schmidt, 1913; Ducrocq, 1997; Holroyd et al., 2010). At present, two anthracothere genera are known from the early Oligocene of the Fayum–*Bothriogenys* Schmidt, 1913 (four species) and *Qatraniodon* Ducrocq, 1997 (one species). Here we describe and discuss an additional new genus that replaces and enhances material previously included in the genus *Rhagatherium* Pictet, 1857. Among other distinguishing features, members of the new taxon are characterized by having a shorter snout, large caniniform canines, and more bunodont cheek teeth, suggesting a more frugivorous and varied diet than for the other, more bunoseledont, Fayum anthracotheres.

Materials and methods

Repositories and institutional abbreviations.—CGM = Cairo Geological Museum; DPC = Duke University Lemur Center, Division of Fossil Primates; NHM = The Natural History Museum, London.

Terminology.—Dental terminology follows that of Lihoreau and Ducrocq (2007). I, C, P, and M (for incisors, canines, premolars, and molars, respectively) are followed by superscript and subscript numbers, referring to upper and lower teeth, respectively. M^{2-3} and M_3 of *Nabotherium* new genus with dental features labeled are illustrated in Figure 3.

Methods.—Ammonium chloride (NH_4Cl) was used to whiten some of the specimens for the photographs presented here. An AF-S micro Nikkor 60-mm f/2.8G ED lens was used to photograph specimens. Stereophotographic figures are presented for some dentitions.

Systematic paleontology

Class Mammalia Linnaeus, 1758
Order Artiodactyla Owen, 1848
Family Anthracotheriidae Leidy, 1869
Subfamily Anthracotheriinae Leidy, 1869
Genus *Nabotherium* new genus
Figures 4–8

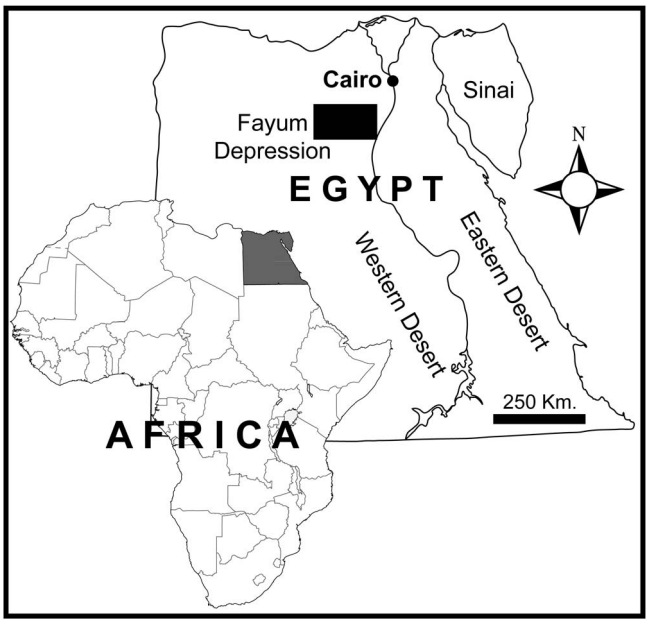

Figure 1. Location of the Fayum Depression in the Western Desert, northern Egypt.

Type species.—*Rhagatherium aegyptiacum* Andrews, 1906, by monotypy.

Diagnosis.—As for the type species.

Etymology.—Combination of *Nab*, Arabic word for canine, in reference to its large upper and lower canines, and *therium,* Greek for wild beast.

Occurrence.—Early Oligocene, Jebel Qatrani Formation, Fayum, Egypt. The holotype of the type species is from an unknown locality in the Jebel Qatrani Formation (Fluvio-Marine Sequence north of Birket Qarun). The referred specimens are from Fayum Quarries A (65-m level), R (210 ml), and V (166 ml) (Fig. 2).

Remarks.—*Nabotherium aegyptiacum* is a new combination. Andrews (1906) proposed the name *Rhagatherium aegyptiacum* for an isolated M^3 (Fig. 4.2) recovered from an unknown locality in the Jebel Qatrani Formation. Andrews (1906) noted that the Fayum specimen was much larger than the two species of *Rhagatherium* known at that time, *R. valdense* Pictet, 1855 and *R. fronstettense* Kowalevsky, 1874, and that when better specimens of the Fayum taxon were found it might be necessary to establish a new genus for them. Other than the material described here, no specimens attributable to '*Rhagatherium*' from the Fayum have come to light in the 100+ years since Andrews (1906).

Hooker and Thomas (2001) provided a thorough review of *Rhagatherium* and associated taxa. *Rhagatherium* was originally described as an anthracothere (Pictet, 1857), and continued to be discussed as one (Stehlin, 1908) for more than 80 years, until Pilgrim (1941) moved it and two other taxa to a new family, Haplobunodontidae. McKenna and Bell (1997) considered the haplobunodontids to be a family within

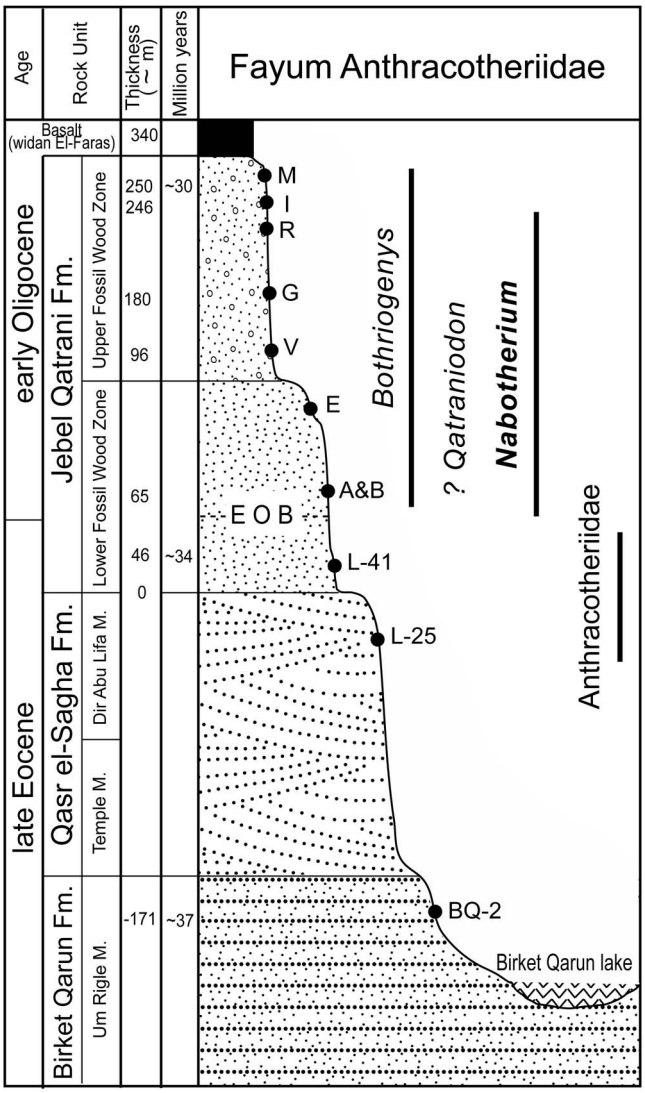

Figure 2. Stratigraphic ranges of Fayum anthracotheres recognized in this paper and unstudied specimens (Anthracotheriidae) from older quarries. Age estimates for major mammal-bearing fossil localities and approximate position of Eocene-Oligocene boundary follow Seiffert (2006).

Anthracotherioidea, although the analysis of Hooker and Thomas (2001) placed *Rhagatherium* as the sister taxon to *Hallebune* Erfurt and Sudre, 1995 within Haplobunodontidae.

DPC 13442 is a left maxilla with P^4–M^2 from Fayum Quarry R (Fig. 4.1) that is very similar to the holotype of *Rhagatherium aegyptiacum* (Fig. 4.2) as described by Andrews (1906). Comparisons between the holotype of *R. aegypticum*, DPC 13442, and Pictet's (1857, pl. 3) illustrations reveal a number of substantial differences between the Fayum specimens and the type material of *R. valdense*, which make clear that the Fayum material does not belong in *Rhagatherium*. For example, *R. valdense* has a P^4 with paired labial cusps (paracone and metacone) that are of the same size and height. These two cusps are connected to a weakly differentiated protocone by a continuous U-shaped crest that incorporates the protocone within it. In contrast, the Fayum taxon has only a single labial cusp, a more distinct protocone, and lacks a postprotocrista.

https://doi.org/10.1017/jpa.2016.13 Published online by Cambridge University Press

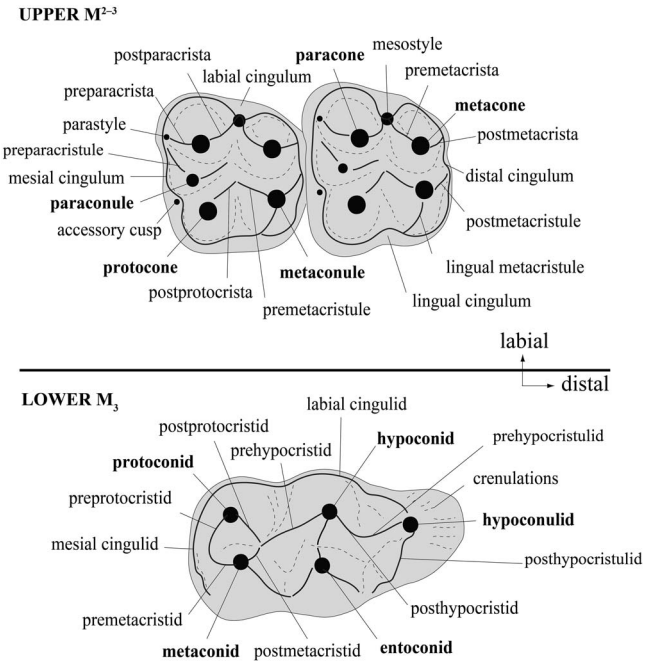

Figure 3. Nomenclature used to describe morphological features of the teeth of *Nabotherium*, following Lihoreau and Ducrocq (2007). Bold face indicates the main cusps of the tooth.

In the molar series, both the Fayum specimens and *Rhagatherium valdense* have upper molars with mesostyles, but in *R. valdense*, the mesostyle is formed as a rounded crest connecting the postparacrista and premetacrista, after each turns labially to form parallel crests that extend nearly to the labial margin of the teeth. Also, the rounded crest forming the mesostylar connection bulges labially so that the labial extent reaches far beyond either the para- or metastylar shelves. In contrast, the Fayum specimens have small, cuspate mesostyles formed by weakly conjoined postpara- and premetacristae that do not run parallel to one another. In addition, the mesostyle does not extend labially beyond the parastyle, and extends only very weakly beyond the metastyle, especially on $M^{2–3}$.

The lower dentition of *Nabotherium aegyptiacum* differs even more substantially from that of *Rhagatherium valdense*. True *Rhagatherium* has marked diastemata between the lower canine and P_2, and between P_2 and P_3. Also, P_1 is absent in *Rhagatherium* but present in *Nabotherium*. All three lower premolars of *Rhagatherium* are elongate and laterally compressed, whereas those of *Nabotherium* are relatively shorter and broader. The molars of *Rhagatherium* are also narrower, and M_1 and M_2 are subequal, unlike in *Nabotherium* and in anthracotheres in general, in which there is normally a size increase in molars from $M^1/_1$ to $M^3/_3$.

These comparisons make it clear that the Fayum taxon '*Rhagatherium*' *aegyptiacum* does not belong in the genus *Rhagatherium* as originally defined by Pictet (1857). To remedy this taxonomic situation, the new generic name *Nabotherium* is here proposed for the species.

Nabotherium aegyptiacum (Andrews, 1906) new combination

1906 *Rhagatherium aegyptiacum* Andrews, p. 192.

Holotype.—NHM M8449, left M^3 (Table 1, Fig. 4.2).

Diagnosis.—Medium-sized anthracothere with dental formula 3.1.4.3.

Differs from contemporaneous *Bothriogenys* in having I^3 caniniform, enlarged caniniform upper and lower canines, very short canine-P^1/P_1 diastema, no diastema between lower canine and I_3, apex of $P^{1–3}$ crowns situated almost midway between the roots, P^1 peg-like and lacking triangular occlusal outline of P^2 and P^3, $P^{2–3}$ mesial and distal crista oriented more mesiodistally rather than obliquely, upper molars with distinctive labial ribs ('barrels') on the labial slopes of the paracone and metacone (see Fig. 4.1–4.3), weakly-developed parastyle and metastyle, mesostyle bulbous and cuspate and not invaded by postparacrista and premetacrista, preparacrista weak and mesially oriented, labial cingula well-developed, strong lingual metacristule connected with lingual cingula, and very weak preprotocristae that never reach the paraconule, and leave a small valley between protocone and paraconule.

Differs from *Qatraniodon* (Andrews, 1906; Ducrocq, 1997) in having much larger tooth dimensions, more bunodont molars that are relatively shorter and broader. Differs from the younger African taxon, *Epirigenys* Lihoreau, Boisserie, Manthi, and Ducrocq, 2015 (see Lihoreau et al., 2015), in lacking a distinct metaconid on P_4, in having a more distinct protocone and shorter pre- and postprotocristae on P^4, and in lacking an enlarged and mesially extended parastylar shelf on upper molars.

Differs from *Anthracothema* Pilgrim, 1928 (see Pilgrim, 1928; Colbert, 1938) in having smaller tooth dimensions; M^2 only slightly smaller than M^3 (M^2 much smaller than M^3 in *Anthracothema*); upper molars with relatively larger and more robust mesostyles; upper molars with complete lingual cingula; $M^{2–3}$ with much smaller anterior cingular cuspule; M_3 with less basally inflated cusps; a more labiolingually constricted trigonid fovea, talonid basin, and hypoconulid fovea; and in possessing a well-developed premetacristid that connects to the preprotocristid, resulting in a closed trigonid basin.

Differs from *Myaingtherium* Tsubamoto, Zin-Maung-Maung-Thein, Egi, Nishimura, Thaung-Htike, and Takai, 2011 (see Tsubamoto et al., 2011) in having a better developed protocone on P^4, P^4 and upper molars with lingual cingula, upper molars with mesostyles, shelf-like parastyles (both absent in *Myaingtherium*), much larger and crestiform paraconules, distinct pre- and postmetacristule (the latter closing off the talon basin distally), and in having distinct and lingually curving paracristids on $P_{2–4}$.

Differs from *Anthracotherium magnum* Cuvier, 1822 (NHM M28770, early Oligocene, Flonheim, Germany) in having less robust and more laterally compressed $I^{2–3}$, a much less robust and more labiolingually compressed upper canine, P^2 with a small protocone shelf, P^3 with a relatively smaller protocone shelf and without a protocone cuspule, M^2 only slightly smaller than M^3, upper molars with complete lingual cingulum, and smaller mesostyles that do not project labially beyond the para- and metastyles, especially on $M^{2–3}$.

Description.—Skull: Due to postmortem damage, the cranium of *Nabotherium aegyptiacum* (CGM 67200; Figs. 5–6) is

https://doi.org/10.1017/jpa.2016.13 Published online by Cambridge University Press

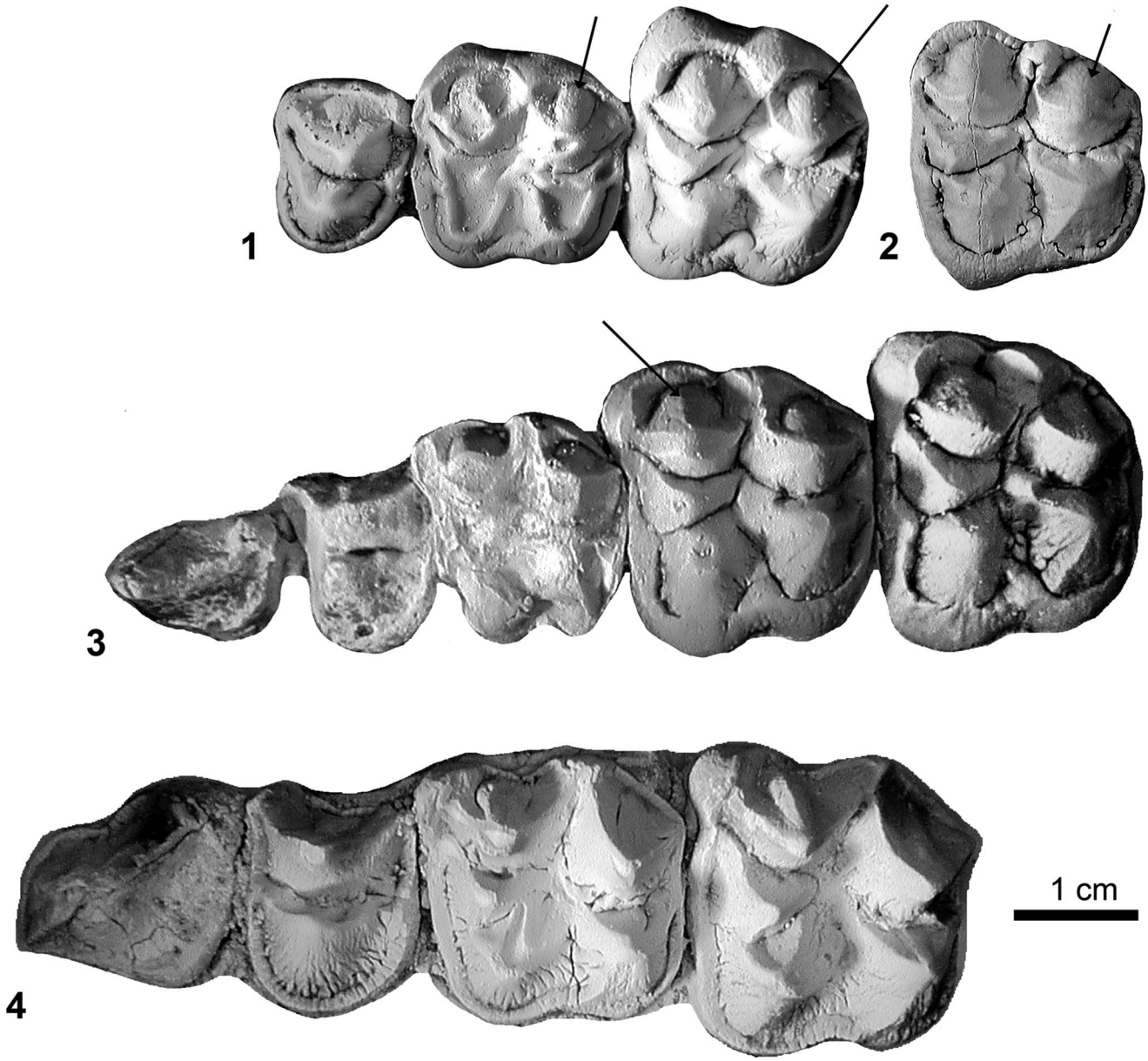

Figure 4. Upper dentitions of *Nabotherium* and *Bothriogenys*. (**1**) Occlusal view of DPC 13442, *N. aegypticum,* left maxilla with P^4–M^2 from Fayum Quarry R. (**2**) Occlusal view of NHM M8449, holotype of *N. aegypticum* (NHM M8449), left M^3 from an unknown horizon in the Jebel Qatrani Formation. (**3**) Occlusal view of DPC 6473, *N. aegyptiacum*, left maxilla with P^3–M^3 from Fayum Quarry V. (**4**) Occlusal view of DPC 4234, *Bothriogenys* sp., left maxilla with P^3–M^2 from Fayum Quarry V. Arrows indicate robust labial ribs ('barrels') of the labial surfaces of the paracone and metacone in *Nabotherium*.

mediolaterally compressed with some morphological features obscured. Also, some of the cranial elements are shifted or appear to be fused together, which makes it difficult to describe some of the bones with confidence. Nonetheless, the specimen reveals many important details about the cranial morphology of *Nabotherium*, and the tooth rows are well preserved, although there are cracks in some places.

The nasal bones are preserved although their relationship with the premaxillae and frontals is obscured. The premaxillae form most of the rostrum (Fig. 5) and preserve alveoli for moderate to large upper incisors. The most rostral part of the premaxillae is damaged but the second and third upper incisors are well preserved, although both are slightly displaced. There are small diastemata separating each incisor. The suture between the premaxilla and the maxilla on the lateral surface of the rostrum is poorly preserved, but it arcs posteriorly above the canines.

The maxillae are severely crushed and the jugal is not preserved. The frontal bones are present and roughly flat. The postorbital process is well developed, short, triangular, and points ventrolaterally from the middle part of the frontal, forming the dorsal arch of the orbit. The length of the postorbital process suggests that the rim of the orbit was open distally. The anterior rim of the orbit is placed above the level between M^2 and M^3. The temporal lines extend posteromedially from the postorbital process to meet at the midline to form the anterior aspect of the sagittal crest.

https://doi.org/10.1017/jpa.2016.13 Published online by Cambridge University Press

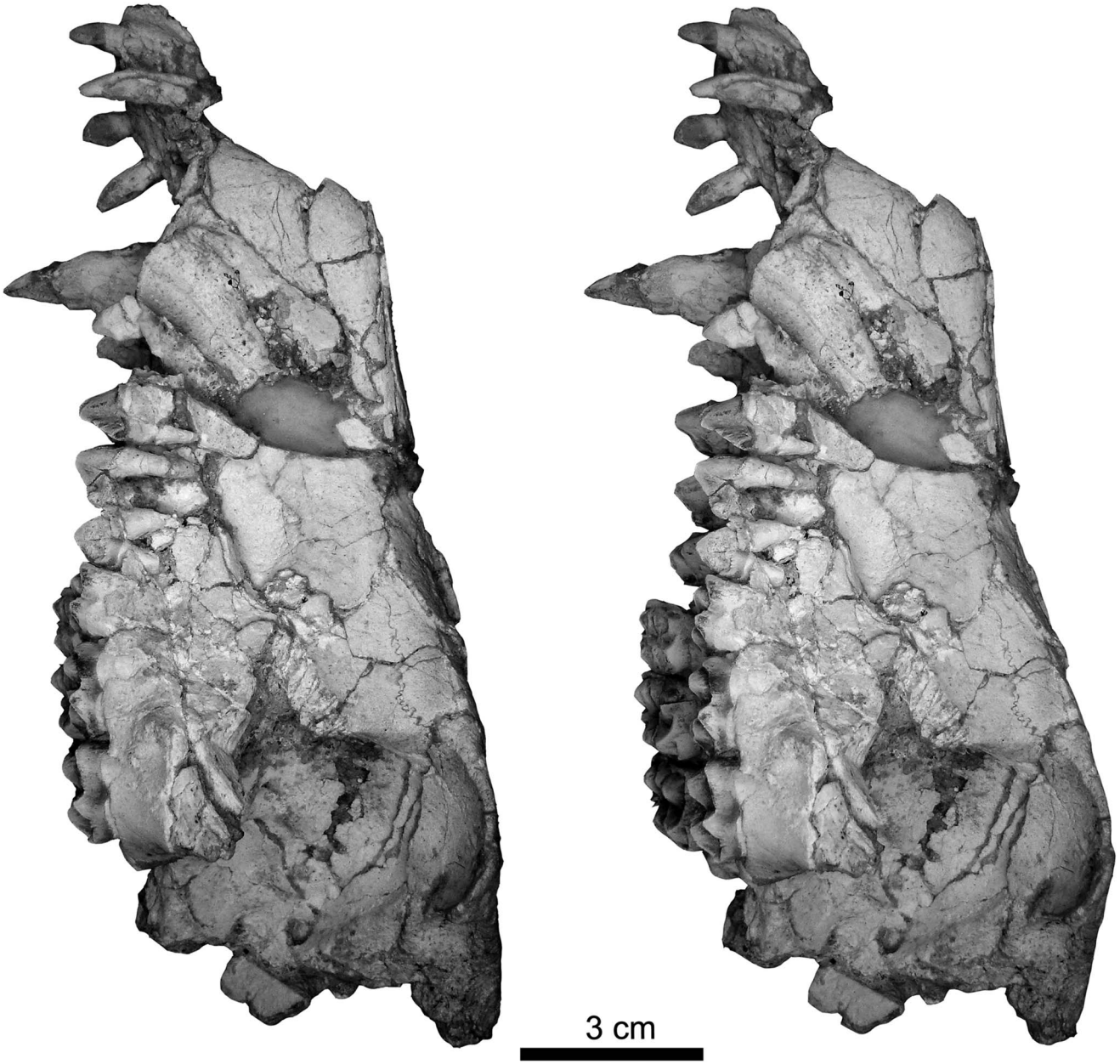

Figure 5. Stereophotographs of a left lateral view of the cranium of *Nabotherium aegyptiacum* (CGM 67200) from Fayum Quarry V, Jebel Qatrani Formation.

Upper dentition: The upper dentition is preserved, except for the first upper incisors and left canine (Fig. 6). The left tooth row is also slightly displaced anteriorly when compared with the right tooth row. The occlusal morphology of the teeth is clear even though minor cracks are visible on the posterior molars. The upper cheek teeth have bunodont crowns, with rounded cusps. The size of the teeth increases from P^1 to M^3.

Upper incisors: I^2 is relatively short and shows a crown that is labiolingually compressed, with a convex labial surface and concave lingual surface. The I^2 mesial and distal crests are sharp and meet at the midpoint of the crown, forming the tip of the tooth. Wear is present on the mesial crest only. The I^3 is narrow and caniniform compared with I^2. The mesial and distal crests are less sharp than on I^2, and an appreciable wear facet is visible on the distal crista. The diastema between I^2 and I^3 is slightly longer than the one between I^1 and I^2.

Upper canines: The upper canine is very large, oval in cross section, being the tallest tooth in the upper dentition, and it has a sharp and pointed tip. The tooth is slightly labiolingually compressed with a deep root that is ~2.5 times bigger than the size of the crown. The mesial part of the tooth is not preserved but the distal edge is well developed. There is a very short diastema between the C and I^3.

Upper premolars: The upper first premolar is relatively small and has two roots. The tooth is peg-like, labiolingually compressed, and triangular in lateral view, being longer than wide and broader distally than mesially. The mesial crest is weakly developed and the distal crest is highly abraded.

https://doi.org/10.1017/jpa.2016.13 Published online by Cambridge University Press

Figure 6. Stereophotographs of the ventral view of the cranium of *Nabotherium aegyptiacum* (CGM 67200), showing the occlusal surface of the dentition.

https://doi.org/10.1017/jpa.2016.13 Published online by Cambridge University Press

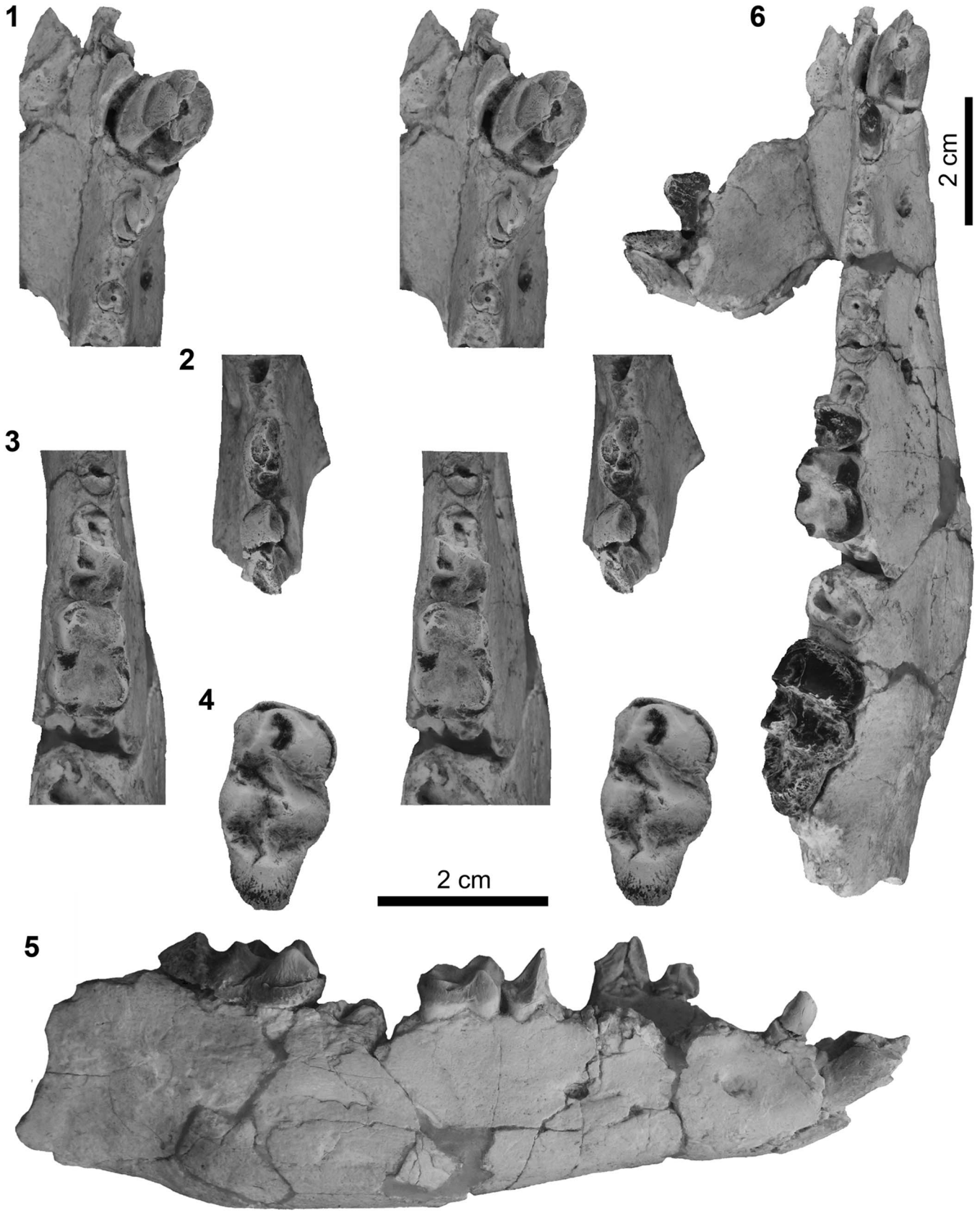

Figure 7. Lower dentition of *Nabotherium aegyptiacum*, CGM 67201. (**1–4**) Stereophotographs of an occlusal surface; (**1**) right C and P_1; (**2**) left $P_{2–3}$; (**3**) right P_4 (broken) and M_1; (**4**) right M_3. (**5**) General labial view. (**6**) General occlusal view.

https://doi.org/10.1017/jpa.2016.13 Published online by Cambridge University Press

Figure 8. Mandibular dentition of *Nabotherium aegyptiacum* in occlusal view. (**1**) DPC 9048, mandible with left C, P_2–M_2, and right C, P_2–M_3 from Fayum Quarry V. (**2**) CGM 67202, left M_3 from Fayum Quarry V.

The occlusal surface bears one main cusp, from which a well-developed distal crest runs labiodistally to terminate at the distolabial base of the crown. There is a very weakly developed cingulum around the base of the crown except along the distal margin. Wear is developed along the tip of the main cusp and the distal crest.

P^2 has a triangular outline, longer than wide, broader distally, and narrower mesially. There are two small inflations along the distal crest course. The mesial crest is very weakly developed when compared with the distal crest. There is a very weakly developed cingulum course around the base of the crown aside from the distal margin. Wear is only found on the tip of the main cusp and along the distal crest. P^3 is essentially identical in morphology to P^2, but differs in being larger and having a relatively large distolingual corner and relatively more robust crests. Distal inflation on the distal crest is also more developed as a minute cusp. There is no parastyle.

P^4 has a roughly ovoid occlusal outline, being broader than long. The tooth has two lobes, with the labial one longer than the lingual one, and two main cusps, paracone and protocone. The protocone is placed slightly mesial to the paracone, and a relatively deep, narrow sinus separates the two cusps. The preparacrista extends mesiolabially from the mesial side of the paracone and fuses with a small accessory cusp on the mesiolabial corner of the crown, from which a short cingulum extends. The postparacrista is shorter than the preparacrista; it runs distolabially from the paracone, and ends as a minor accessory cusp on the distolabial corner of the tooth. On the distal margin of the crown, there is an additional small cusp.

Upper molars: M^1 is the smallest molar with M^2 being either smaller than or nearly equal in size to M^3. M^1 (Fig. 6) is the most worn tooth in the upper dentition, although it is clear that the tooth has a semiquadrate occlusal outline, with a relatively short lingual margin and a broader mesial margin. The four main cusps of the crown (paracone, protocone, metacone, and metaconule) are all approximately equal in size. There is a distinct paraconule situated lingual to the paracone. A well-developed cuspate mesostyle is present and is centered on the labial wall of the tooth. On the labial wall of M^1, a low and well-developed labial cingulum runs mesially from the base of the mesostyle to merge with the mesial cingulum, forming a shelf around the mesiolabial corner of the crown. There is also a more weakly developed cingulum originating at the base of the mesostyle and tapering around the distolabial corner of the tooth. In the mesiolabial corner of the crown, there is a minute parastyle visible as a small inflation, which is connected distally to the paracone via a very weakly developed preparacrista. The postparacrista and premetacrista run distolabially and mesiolabially, respectively, and meet each other at the lingual base of the mesostyle. The mesial cingulum is well developed, and runs lingually from the parastyle to terminate at the mesiolingual base of the protocone.

M^2 is similar to M^1 in its occlusal morphology, but differs in being larger and having relatively more robust cusps and cristae, and in having a relatively narrower distal portion. The right M^2 is affected by minor cracking. The paraconule is well developed, slightly mesially placed between the paracone and protocone, tapers distally, and ends at the midline of the crown. It is separated from the paracone and protocone by narrow and shallow grooves, the labial of which is wider than the lingual. Mesially, there is a short preparacristule that extends from the mesiolabial part of the paraconule to merge with the lingual base of the parastyle. There is an accessory cusp on the mesial cingulum situated mesiolabially to the protocone.

The metaconule bears three cristae. The premetacristule runs mesiolabially to merge with the postprotocrista, forming an inverted V-shape in the middle of the transverse valley of the crown.

https://doi.org/10.1017/jpa.2016.13 Published online by Cambridge University Press

Table 1. Tooth measurements of the hypodigm of *Nabotherium aegypticum* n. gen. (length x width, in mm).

Specimen	Canine	P^1	P^2	P^3	P^4	M^1	M^2	M^3
Upper Dentition								
NHM M8449	–	–	–	–	–	–	–	17.1 × 19.5
DPC 13442	–	–	–	–	9.9 × 12.2	15.3 × 15.8	16.9 × 20.9	–
CGM 67200	11.2 × 8.6	7.2 × 4.2	11.5 × 7.6	13.1 × 9.5	11.6 × 12.4	14.6 × 14.9	18.3 × 19.7	18.7 × 21.6
DPC 6473	–	–	–	13.3 × 8.9	11.4 × 13.3	–	18.8 × 20.7	19.4 × 22.8
DPC 8213	–	–	–	–	10.8 × 12.7	13.9 × 15.3	17.4 × 19.8	18.3 × 21.5
DPC 8410	11.3 × 8.9	–	–	–	–	–	–	–
DPC 10527	–	–	–	–	12.6 × 13.8	–	–	–
DPC 10825	–	–	–	–	12.1 × 14.2	15.2 × 16.9	16.1 × 19.8	18.2 × 22.5
Lower Dentition								
CGM 67201	10.3 × 9.7	7.3 × 3.6	10.6 × 5.1	–	–	15.9 × 10.9	–	28.4 × 15.7
CGM 67202	–	–	–	–	–	–	–	31.0 × 15.2
DPC 9048	12.5 × 10.2	–	10.3 × 5.3	12.7 × 6.8	12.9 × 9.0	14.4 × 12.1	17.4 × 13.8	–
DPC 10197	–	–		–	–	–	–	29.4 × 15.0
DPC 10668	–	–	10.3 × 5.2	–	13.3 × 8.5	–	–	28.9 × 14.1
DPC 10736	–	–	–	–	–	16.1 × 10.9	–	–
DPC 13424	–	–	–	–	18.9 × 10.1	18.1 × 11.5	21.8 × 14.6	–

The postmetacristule runs distolabially and fuses with the distal cingulum; and the lingual metacristule runs mesiolingually to merge with the lingual cingulum.

The occlusal pattern on M^3 is similar to those observed on M^1 and M^2. M^3 is larger although with a relatively shorter distal margin, giving the tooth a somewhat trapezoidal occlusal outline. Also, the parastyle is less developed on M^3 than on M^2. A weakly developed preparacrista is present. The cingulum is continuous around the crown. The labial cingulum is well developed with respect to that of M^2, in particular the portion labial to the paracone.

Mandible: *Nabotherium aegyptiacum* has a robust mandible with a relatively shallow horizontal ramus. Although CGM 67201 (Fig. 7) shows numerous fractures due to postmortem damage, three mental foramina are visible. The mesial mental foramen has a roughly oval outline and is situated below the mesial root of P_2. The distal mental foramen is roughly the same size as the mesial one and is positioned between P_3 and P_4. The third mental foramen is situated below the mesial root of P_3. The mandibular symphysis is fused in adults, U-shaped, and extends posteriorly back to the level of P_2.

Lower dentition: The anterior portion of the mandible in CGM 67201 is distorted and the lower incisors are not preserved. However, DPC 9048 (Fig. 8) preserves this region (although not the incisors themselves) and makes clear that *Nabotherium* had three lower incisors on each side arranged in a shallow arc across the front of the mandible, and that I_3 was not separated from the canine by a diastema. The canines are large, projecting, and oval in cross section.

In CGM 67201, the alveolus of the left lower canine is exposed, which reveals that the tooth root is very deep and curves dorsally to terminate beneath P_1. DPC 9048 has both canines in place and shows that the mesial edge of the canine is sharply defined, and that a wear facet is present on the distal canine surface.

Lower premolars: P_1 is a small peg-shaped tooth with a labiolingually compressed crown and an oval base, and is separated by a very short diastema from the lower canine. In CGM 67201(Fig. 7), the right P_1 is well preserved and consists of one main cusp, from which run mesial and distal cristids, the distal one being longer than the mesial one. The tooth is single-rooted, convex laterally, concave medially, and curves distally. There is a short diastema between the P_1 and P_2, slightly larger than that between the P_1 and the canine.

The left P_2 is well preserved in both CGM 67201 and DPC 9048 (Figs. 7.2, 8.1). The tooth is larger than P_1, triangular in shape when viewed lingually, and double-rooted. The main cusp is tall and acutely pointed. A cristid runs mesially from the main cusp to terminate at the base of the crown. The distal cristid runs distally from the distal portion of the main cusp and bifurcates into two cristids, one of which runs lingually and the other continues distally to end at the base of the crown, meeting the small and shallow distal cingulid. The latter cristid courses around the distal margin of the tooth. There is no diastema between the P_2 and P_3.

P_3 is well-preserved on DPC 9408. It has a morphology similar to that of P_2, but it is larger with a more distinct and relatively longer mesial crest and a more distally extended posterior portion.

P_4, best observed on DPC 9048, is relatively more robust and broader than the other premolars. The P_4 protoconid is as high as those of $P_{2–3}$ and is more robust. The mesial crest is slightly more curved than that of P_3 and the lingual distal crest is stronger. The distal portion of the crown is relatively broader than in the other premolars and a low shelf is formed by an expanded distal cingulid.

Lower molars: M_1 is relatively long and broad when compared with P_4 and shows appreciable wear compared to other cheek teeth. The second lower molar is well preserved in DPC 9048 and is a slightly longer and broader version of M_1 but with a broader (mesiodistally) hypoconulid shelf.

M_3 is the longest lower molar because it has an extended hypoconulid lobe (Figs. 7.4, 8.1–8.2). The M_3 trigonid and talonid are equally wide and have crenulations covering the occlusal surface. The mesial cingulid is moderately developed, runs around the mesial margin of the crown, and merges with the labial cingulid. There is a small spur on the mesial cingulid at the base of metaconid. The metaconid and protoconid are transversely placed and separated by a deep and narrow valley. The premetacristid slopes down from the mesial side of the metaconid and joins the preprotocristid near the middle of the mesial margin of the tooth, forming a U-shaped crest.

The hypoconid is placed slightly mesial to the entoconid. The prehypocristid (cristid obliqua) is acute and curves

https://doi.org/10.1017/jpa.2016.13 Published online by Cambridge University Press

mesiolingually to merge with the distal junction between the postmetacristid and postprotocristid. There is no postentocristid and the posthypocristid run distolingually from the hypoconid to merge with the prehypocristulid that slopes down from the hypoconulid, leaving the longitudinal valley open. The hypoconulid is a distinct cusp, occupies the central part of the distal margin of the crown, and forms a very distinct third lobe. The posthypocristulid runs from the hypoconulid summit to end at the base of the entoconid. In labial view, a hypocristulid slopes mesiolabially toward the base of the hypoconid to merge with the labial cingulid. Occasionally there is a small knob developed on the posthypocristulid at the base of the hypoconid.

Materials.—From Quarry A: 13424, mandible with symphysis, left $M_{1–2}$ and right broken P_3–M_1 and $M_{2–3}$. From Quarry R: DPC 13442 (Fig. 4.1), left maxilla with P^4–M^2. From Quarry V: CGM 67200, a laterally crushed skull that preserves the upper dentition (right and left $I^{2–3}$, C, $P^{1–4}$, $M^{1–3}$), except right and left I^1 and left C (Table 1, Figs. 5–6); CGM 67201 (Fig. 7), right dentary with C, P_1, P_4 (broken), M_1, M_3, and left dentary with P_2–P_3; CGM 67202 (Fig. 8.2), left dentary fragment preserving M_3 and part of the distal root of M_2; DPC numbers: 6473 (Fig. 4.3), left maxilla with P^3–M^3; 8213, left maxilla P^4–M^3; 8410, left upper C; 9048 (Fig. 8.1), mandible with left and right C, P_2–M_3; 10197, left dentary with M_3; 10527, left P^4; 10668, right dentary with M_2 (broken), M_3; 10736, mandible with left $dI_{1–3}$, dC, $dP_{1–4}$, M_1 and right $dP_{3–4}$, M_1; 10825, palate with left P^4–M^3, right P^4–M^2.

Comparison.—Members of *Nabotherium* exhibit a suite of distinctive features not seen among the other Fayum anthracotheres. *Nabotherium* differs from *Bothriogenys* in ways that suggest utilization of differing diets. *Nabotherium* has more bunodont and generally broader cheek teeth. The front of the skull is shortened and it lacks a canine-premolar diastema. *Nabotherium* possesses large, projecting, and relatively laterally compressed canines that are oval in cross section. In the upper molar row, *Nabotherium* differs from other Fayum anthracotheres in a large number of occlusal details, including the presence of cuspate mesostyles, well-developed labial and lingual cingula, distinctive labial surfaces of the para- and metacones (compare Fig. 4.1, 4.3 with 4.4) that have very strong barrels, and a well-developed lingual metacristule that joins with the lingual cingulum. This is combined with only weakly developed parastyles, metastyles, preparacristae, and postmetacristae.

One specimen assigned to *Nabotherium aegyptiacum* from Fayum Quarry A (DPC 13424) differs from other known specimens of this taxon in having more robust and larger premolars, and somewhat larger molars (Table 1). It is not clear whether these features might be taxonomically meaningful or whether they are better interpreted as representing idiosyncratic variation, but the specimen is assigned to *N. aegyptiacum* because, other than relatively larger tooth size, it is morphologically comparable to other members of the species.

Relatively little can be said about the differences between *Nabotherium* and *Qatraniodon*, due to the fact that *Qatraniodon* is not very well known, and the type preserves only $M_{1–2}$. However, *Nabotherium* is clearly distinct from *Qatraniodon* in being larger and in having much more bunodont and relatively wider molars. *Qatraniodon* has a small and low, but distinct, cingular spur on M_1 that is lacking in *Nabotherium*, and the posterior shelves of $M_{1–2}$ in *Nabotherium* are relatively broader than in *Qatraniodon*.

Nabotherium further differs from the Asian Paleogene anthracotheres including: *Siamotherium* Suteethorn, Buffetaut, Helmcke-Ingavat, Jaeger, and Jongkanjanasoontorn, 1988, *Anthracokeryx* Pilgrim and Cotter, 1916, and *Anthracohyus* Pilgrim and Cotter, 1916. Specifically, *Nabotherium* differs from *Siamotherium* in having a double rooted P^1, and in having a well-developed lingual metacristule continuous with the lingual cingulum, a distolabially oriented paraconule, and more distinct mesostyles on the upper molars.

The Egyptian taxon differs from *Anthracokeryx* (Colbert, 1938) in lacking diastemata between the lower canine–P_1, P_1–P_2, and P_2–P_3, in having relatively shorter and broader cheek teeth, and in having a (albeit small) P^2 protocone shelf.

Nabotherium is distinct from *Anthracohyus* (known only from a single upper molar; Colbert, 1938) in having a bulbous, cuspate mesostyle (*Anthracohyus* has only a tiny crest in the position of the mesostyle), a better developed parastylar area, distinct labial barrels on the labial surfaces of the paracone and metacone, and a distinct lingual cingulum.

Discussion

Anthracotheres have long been recognized as a family of artiodactyls that likely originated in North America or Eurasia, at least by the late middle Eocene, and subsequently spread and diversified throughout Laurasia and Africa (Lihoreau and Ducrocq, 2007). The oldest known definitive anthracotheres have been identified from deposits in North America (ca. 42 Ma) and Myanmar (Burma) (ca. 40 Ma) (Khin Zaw et al., 2014), and although the origin of African anthracotheres is uncertain, their ancestry can probably be traced to a Eurasian form that reached Africa during or before the late Eocene.

Three anthracothere lineages are known from the early Oligocene deposits of the Fayum: a bunodont form (*Nabotherium*), and two bunoselenodont ones (*Bothriogenys, Qatraniodon*). This same pattern, of coexisting bunodont and bunoselenodont lineages, seems to be fairly common; it has been noted previously among Eurasian and North American faunas (Macdonald, 1956; Lihoreau and Ducrocq, 2007) and is now documented in Africa as well.

Of the bunoselenodont forms, *Qatraniodon* is known from only a single specimen, which is a lower jaw with two molars. However, *Bothriogenys* is well represented in the Fayum faunal assemblage and exhibits features that include relatively longer and narrower cheek teeth, more complex premolars often with accessory crest development, occasional supernumerary teeth (GFG, ERM, personal observations), more complex molar teeth, with high crowns that sometimes show development of neomorphic crests and cuspules, and small, more incisiform canines, combined with a long anterior canine-premolar diastema, and a mandibular symphysis that is canted anteriorly, resulting in an elongated, scoop-like anterior dental arcade. Dental adaptations such as these are typically seen in browsing

https://doi.org/10.1017/jpa.2016.13 Published online by Cambridge University Press

and grazing herbivores and it is likely that *Bothriogenys* focused on foliage. In particular, given the apparent hydrophyllic nature of some anthracotheres (Pickford, 2008), *Bothriogenys* might have relied on aquatic plants as dietary staples. *Nabotherium*, in contrast, with its relatively shorter rostrum, enlarged projecting canines, short to absent anterior diastemata, low-crowned and simple premolars, and low, broad, bunodont molars, was likely to have been a more eclectic frugivore/herbivore.

Acknowledgments

We thank O. Teamaa, chairman of Egyptian Mineral Resources Authority, S. Mansour, director of the Central Administration at the Egyptian Geological Survey, R. Hraoun, general director of Egyptian Geological Museum, and M. Abdel Ghani, curator of invertebrate Paleontology Collections in the Egyptian Geological Museum, for facilitating this work. We would like to thank S. El-Sayed and I. El Dawoudi from Mansoura University Vertebrate Paleontology Center (MUVP) for assistance with preparation and other aspects of the research. Two anonymous reviewers helped to improve a previous version of this paper.

References

Andrews, C.W., 1906, A descriptive catalogue of the Tertiary Vertebrata of the Fayum, Egypt. Based on the collection of the Egyptian government in the Geological Museum, Cairo, and on the collection in the British Museum (Natural History), London: London, British Museum of Natural History, 324 p.

Colbert, E.H., 1938, Fossil Mammals from Burma in the American Museum of Natural History: Bulletin of the American Museum of Natural History, v. 74, p. 255–436.

Cuvier, G., 1822, Recherches sur les Ossemens Fossils, où l'on Rètabit les Caractères de Plusieurs Animax don't les Revolutions du Globe ont Détruit les Espèces: Paris, Dufour et E. d'Ocagne, 412 p.

Domning, D.P., and Gingerich, P.D., 1994, *Protosiren smithae*, new species (Mammalia, Sirenia), from the late middle Eocene of Wadi Hitan, Egypt: Contributions from the Museum of Paleontology, University of Michigan, v. 29, p. 69–87.

Domning, D.P., Gingerich, P.D, Simons, E.L., and Ankel-Simons, F.A., 1994, A new early Oligocene dugongid (Mammalia, Sirenia) from Fayum Province, Egypt: Contributions from the Museum of Paleontology, University of Michigan, v. 29, p. 89–108.

Ducrocq, S., 1997, The anthracotheriid genus *Bothriogenys* (Mammalia, Artiodactyla) in Africa and Asia during the Paleogene: Phylogenetical and paleobiogeographical relationships: Stuttgarter Beitrage zur Naturkunde, B (Geologie und Palaontologie), v. 250, p. 1–44.

Erfurt, J., and Sudre, J., 1995, Un Haplobunodontidae nouveau, *Hallebune krumbiegeli* nov. gen. nov. sp. (Artiodactyla, Mammalia), dans l'Eocene moyen du Geiseltal pres halle (Sachsen-Anhalt, Allemagne): Palaeovertebrata, v. 24, p. 84–99.

Gingerich, P.D., Smith, B.H., and Simons, E.L., 1990, Hind limbs of Eocene *Basilosaurus isis*: Evidence of feet in whales: Science, v. 249, p. 154–157.

Holroyd, P., Lihoreau, P., Gunnell, G.F., and Miller, E.R., 2010, Anthracotheriidae, *in* Werdelin, L., and Sanders, W.J., eds., Cenozoic Mammals of Africa: Berkeley, University of California Press, p. 843–851.

Hooker, J.J., and Thomas, K.M., 2001, A new species of *Amphirhagatherium* (Choeropotamidae, Artiodactyla, Mammalia) from the late Eocene Headon Hill Formation of southern England and phylogeny of endemic European 'anthracotherioids': Palaeontology, v. 44, p. 827–853.

Khin, Zaw, Meffre, S., Takai, M., Suzuki, H., Burrett, C., Thaung, Htike, Zin, Maung, Maung, Thein, Tsubamoto, T., Egi, N., and Maung Maung, 2014, The oldest anthropoid primates in SE Asia: Evidence from LA-ICP-MSU-Pb zircon age in the late middle Eocene Pondaung Formation, Myanmar: Gondwana Research, v. 26, p. 122–131.

Kowalevsky, W., 1874, Monographie der Gattung *Anthracotherium*: Palaeontographica, v. 22, p. 131–290.

Leidy, J., 1869, The extinct mammalian fauna of Dakota and Nebraska, including an account of some allied forms from other localities, together with a synopsis of the mammalian remain of North America: Journal of the Academy of Natural Sciences, Philadelphia, ser. 2, v. 7, p. 1–472.

Lihoreau, F., and Ducrocq, S., 2007, Family Anthracotheriidae, *in* Prothero, D.R., and Foss, S.E., eds., The Evolution of Artiodactyls, Baltimore, Maryland, The Johns Hopkins University Press, p. 89–105.

Lihoreau, F., Boisserie, J.R., Manthi, F.K., and Ducrocq, S., 2015, Hippos stem from the longest sequence of terrestrial cetartiodactyl evolution in Africa: Nature Communications, v. 6, p. 6264, doi:10.1038/ncomms7264.

Linnaeus, C., 1758, Systema Naturae per Regna tria Naturae, secundum Classes, Ordines, Genera, Species, cum Characteribus, Differentis, Synonymis, Locis, 10th ed., Stockholm, Sweden, Laurentii, Slavi, 824 p.

Macdonald, J.R., 1956, The North American anthracotheres: Journal of Paleontology, v. 30, p. 615–645.

McKenna, M.C., and Bell, S.J., 1997, Classification of Mammals Above the Species Level: New York, Columbia University Press, 631 p.

Murray, A.M., Cook, T.D., Attia, Y.S., Chatrath, P., and Simons, E.L., 2010, A freshwater ichthyofauna from the late Eocene Birket Qarun Formation, Fayum, Egypt: Journal of Vertebrate Paleontology, v. 30, p. 665–680.

Owen, R., 1848, Description of teeth and portions of two of two extinct anthracotheroid quadrapeds (*Hyopotamus vectianus* and *H. bovinus*) discovered by the Marchioness of Hastings in the Eocene deposits on the N.W. coast of the Isle of Wight, with an attempt to develop Cuvier's idea of the classification of pachyderms by the number of their toes: Quarterly Journal of the Geological Society of London, v. 4, p. 104–141.

Pickford, M., 2008, *Libycosaurus petrocchii* Bonarelli, 1947, and *Libycosaurus anisae* (Black, 1972) (Anthracotheriidae, Mammalia): Nomenclatural and geochronological implications: Annales de Paléontologie, v. 94, p. 39–55.

Pictet, F.J., 1855–1857, Mémoire sur les Animaux Vertébrés Trouvés dans le Terrain Sidérolitique du Canton de Vaud et Appartenant a la Faune Éocene, Seconde Partie, Description des Ossements Fossiles: Geneva, Switzerland, J. Kessman, Libraire, p. 27–120.

Pictet, F.J., 1857, Seconde Partie. Description des ossements fossiles trouvés au Mauremont, *in* Pictet, F.-J., Gaudin, C., and De La Harpe, P. 1855–1857, Mémoire sur les Animaux Vertébrés Trouvés dans le Terrain Sidérolithique du Canton de Vaud et Appartenant à la Faune Éocène, Volume 2, Matériaux de Paléontologie Suisse (note 1), Geneva, Switzerland, J. Kessmann, p. 27–120.

Pilgrim, G.E., 1928, The Artiodactyla of the Eocene of Burma: Palaeontologia Indica, v. 13, p. 1–39.

Pilgrim, G.E., 1941, The dispersal of the Artiodactyla: Biological Reviews, v. 16, p. 134–163.

Pilgrim, G.E., and Cotter, G.D., 1916, Some newly discovered Eocene mammals from Burma: Records of the Geological Survey of India, v. 47, p. 42–77.

Rasmussen, D.T., and Simons, E.L., 1988, New Oligocene hyracoids from Egypt: Journal of Vertebrate Paleontology, v. 8, p. 67–83.

Sallam, H.M., Seiffert, E.R., Steiper, M.E., and Simons, E.L., 2009, Fossil and molecular evidence constrain scenarios for the early evolutionary and biogeographic history of hystricognathous rodents: Proceedings of the National Academy of Sciences, v. 106, p. 16722–16727.

Sallam, H.M., Seiffert, E.R., and Simons, E.L., 2011, Craniodental morphology and systematics of a new family of hystricognathous rodents (Gaudeamuridae) from the late Eocene and early Oligocene of Egypt: PLoS ONE, v. 6, e16525.

Schmidt, M., 1913, Ueber Paarhufer der fluviomarinen Schichted des Fajum: Geologische und Paläontologische Abhandlungen, v. 15, p. 153–264.

Seiffert, E.R., 2006, Revised age estimates for the later Paleogene mammal faunas of Egypt and Oman: Proceedings of the National Academy of Sciences, v. 103, p. 5000–5005.

Seiffert, E.R., 2007, A new estimate of afrotherian phylogeny based on simultaneous analysis of genomic, morphological, and fossil evidence: BMC Evolutionary Biology, v. 7, p. 224, doi:10.1186/1471-2148-7-224.

Seiffert, E.R., 2010, The oldest and youngest records of afrosoricid placentals from the Fayum Depression of northern Egypt: Acta Palaeontologica Polonica, v. 55, p. 599–610.

Seiffert, E.R., 2012, Early primate evolution in Afro-Arabia: Evolutionary Anthropology, v. 21, p. 239–253.

Seiffert, E.R., Simons, E.L., and Attia, Y., 2003, Fossil evidence for an ancient divergence of lorises and galagos: Nature, v. 422, p. 421–424.

Seiffert, E.R., Perry, J.M.G., Simons, E.L., and Boyer, D.M., 2009, Convergent evolution of anthropoid-like adaptations in Eocene adapiform primates: Nature, v. 461, p. 1118–1121.

Simons, E.L., and Rasmussen, D.T., 1990, Vertebrate paleontology of Fayum: History of research, faunal review and future prospects, *in* Said, R., ed., The Geology of Egypt: Rotterdam, The Netherlands, A. A. Balkema, p. 627–638.

Simons, E.L., Seiffert, E.R., Ryan, T.M., and Attia, Y., 2007, A remarkable female cranium of the early Oligocene anthropoid *Aegyptopithecus zeuxis* (Catarrhini, Propliopithecidae): Proceedings of the National Academy of Sciences, v. 104, p. 8731–8736.

Stehlin, H.G., 1908, Die Säugethiere des Schweizerischen Eocaens. Critischer Catalog der Materialien. 5. *Choeropotamus—Cebochoerus—Choeromorus—Haplobunodon—Rhagatherium—Mixotherium*: Abhandlungen Schweizerischen Paläontologischen Gesellschaft, v. 35, p. 691–837.

Suteethorn, V., Buffetaut, E., Helmcke-Ingavat, R., Jaeger, J.J., and Jongkanjanasoontorn, Y., 1988, Oldest known Tertiary mammals from Southeast Asia: Middle Eocene primate and anthracotheres from Thailand: Neues Jahrbuch für Geologie und Paläontologie Monatshefte, v. 9, p. 563–570.

Tsubamoto, T., Zin-Maung-Maung-Thein, Egi, N., Nishimura, T., Thaung-Htike, and Takai, M., 2011, A new anthracotheriid artiodactyl from the Eocene Pondaung Formation of Myanmar: Vertebrat Palasiatica, v. 49, p. 85–113.

Accepted 26 July 2015

https://doi.org/10.1017/jpa.2016.13 Published online by Cambridge University Press